Analysis of gene expression in microglial apoptotic cell clearance following spinal cord injury based on machine learning algorithms

LEI YAN*, CHU CHEN*, LINGLING WANG*, HONGXIANG HONG, CHUNSHUAI WU, JIAYI HUANG, JIAWEI JIANG, JIAJIA CHEN, GUANHUA XU and ZHIMING CUI

The First People's Hospital of Nantong, The Second Affiliated Hospital of Nantong University, Research Institute for Spine and Spinal Cord Disease of Nantong University, Nantong, Jiangsu 226019, P.R. China

Received November 1, 2023; Accepted April 17, 2024

DOI: 10.3892/etm.2024.12581

Abstract. Spinal cord injury (SCI) is a severe neurological complication following spinal fracture, which has long posed a challenge for clinicians. Microglia play a dual role in the pathophysiological process after SCI, both beneficial and detrimental. The underlying mechanisms of microglial actions following SCI require further exploration. The present study combined three different machine learning algorithms, namely weighted gene co-expression network analysis, random forest analysis and least absolute shrinkage and selection operator analysis, to screen for differentially expressed genes in the GSE96055 microglia dataset after SCI. It then used protein-protein interaction networks and gene set enrichment analysis with single genes to investigate the key genes and signaling pathways involved in microglial function following SCI. The results indicated that microglia not only participate in neuroinflammation but also serve a significant role in the clearance mechanism of apoptotic cells following SCI. Notably, bioinformatics analysis and lipopolysaccharide + UNC569 (a MerTK-specific inhibitor) stimulation of BV2 cell experiments showed that the expression levels of Anxa2, Myo1e and Spp1 in microglia were significantly upregulated following SCI, thus potentially involved in regulating the clearance mechanism of apoptotic cells. The present study suggested that Anxa2, Myo1e and Spp1 may serve as potential targets for the future treatment of SCI and provided a theoretical basis for the development of new methods and drugs for treating SCI.

Correspondence to: Professor Zhiming Cui, The First People's Hospital of Nantong, The Second Affiliated Hospital of Nantong University, Research Institute for Spine and Spinal Cord Disease of Nantong University, 666 Shengli Road, Chongchuan, Nantong, Jiangsu 226019, P.R. China
E-mail: cuizhiming3425222@163.com

*Contributed equally

Key words: weighted gene co-expression network analysis, random forest analysis, least absolute shrinkage and selection operator analysis, protein-protein interaction, spinal cord injury, microglia, apoptotic cells, machine learning, bioinformatics

Introduction

Spinal cord injury (SCI) is a severe complication of spinal fractures, where the spinal cord or cauda equina sustains varying degrees of damage due to vertebral displacement or bone fragments invading the spinal canal (1). The necrotic and apoptotic cells at the site of SCI release various neuroinflammatory signals recruiting local and infiltrating immune cells and regulating inflammatory cascade reactions. Sensory, motor and autonomic dysfunction caused by SCI leaves patients unable to care for themselves, resulting in a significant economic burden on their family and on society (2). Despite significant advances in medical care for SCI, it remains a challenge for clinical physicians for a number of years and current treatment plans primarily focus on providing supportive measures (3,4).

Microglia are permanent immune cells widely distributed in the central nervous system (CNS), contributing to the maintenance of neuronal function and playing a crucial role in phagocytosis, immune regulation and neural repair (5). Under physiological conditions, microglia can actively monitor the CNS environment and respond to disruptive signals, clearing cell debris and modulating synaptic transmission (6). The microglial population is dynamic in regulating the innate immune response of the CNS (7). Additionally, the functional phenotype of microglia varies when different regions of the CNS are damaged (8,9). Compared with neurotrauma in brain regions, microglia play a more pronounced dual role in the pathophysiological processes following SCI, acting both beneficially and harmfully (10). In the early stages of SCI, microglia rapidly gather around the lesion to provide protection, but with the continued accumulation of injury factors, over-activated microglia produce harmful substances, exacerbating spinal cord tissue damage and affecting functional recovery (11). Although numerous studies demonstrate the crucial role of microglia post-SCI (10-14), the potential mechanisms require further exploration.

Microglia are macrophages resident in the CNS, maintaining tissue homeostasis through phagocytosis (15). The apoptotic cell clearance is the final step in efferocytosis (16).

Efferocytosis mainly comprises four steps: Identification of apoptotic cells, recognition of apoptotic cells adjacent to engulfing cells, internalization of apoptotic cells by engulfing cells and degradation of apoptotic cells within engulfing cells (17). Multiple signaling molecules cooperate to regulate the entire phagocytic clearance process, from 'find me' signals to 'eat me' signals and beyond (18). The distinct expression of apoptotic cell surface markers initiates the migration and recognition of early phagocytic cells, triggering timely and efficient phagocytosis to avoid inflammation spreading or to maintain homeostatic balance (19). The clearance of apoptotic cells by microglia not only serves a significant neuroprotective role in degenerative diseases (20) but also has positive effects in neuronal death and clearance in acute brain trauma (21) and brain ischemia-hypoxia (22). Despite the considerable attention focused on efferocytosis, the mechanisms of microglial clearance of apoptotic cells following SCI have been overlooked and require further research for clarification.

Bioinformatics, as a practical interdisciplinary field combining molecular biology and information technology, has partially revealed the potential mechanisms of diseases at the molecular level, providing new avenues for the diagnosis and treatment of human diseases (23). High-throughput chip sequencing technology rapidly captures differential gene expression profiles and efficiently acquires biological information on a large scale and is widely employed in basic medical research and disease diagnostics (24). Machine learning refers to a category of algorithms aiming to extract hidden rules from extensive historical data for prediction or classification purposes (25). Due to the expanding scale of biological data and the inherent complexity of machine learning, it has been widely and deeply applied in bioinformatics to aid in establishing predictive and analytical models explaining potential biological processes (25). Innovations in technologies such as high-throughput sequencing have brought new advancements in the study of microglial heterogeneity (26). The present study aimed to explore the mechanism of apoptosis clearance of microglia post-SCI using various machine-learning algorithms.

Mertk, a member of the TAM (Tyro3, Axl, Mertk) receptor tyrosine kinase family, is primarily expressed by microglial cells (27,28). A number of studies indicate that Mertk regulates the phagocytic clearance of apoptotic cells and myelin debris by microglia and macrophages (29-31). UNC569 is an ATP-competitive, reversible, orally active MerTK-specific inhibitor that can inhibit the clearance function of microglia (32). It is well-known that stimulating microglia with lipopolysaccharide (LPS) can simulate neuroinflammation in microglia (33-35), with multiple studies demonstrating the feasibility of this method (36-39).

The present study comprehensively analyzed the data from GSE96055 (40) using various machine learning algorithms and bioinformatics tools to uncover the crucial mechanisms and key genes of microglia involved in SCI and experimentally validate them through treatment with LPS + UNC569 on the BV2 cell line. The present study provided unique insights into the mechanisms through which microglia regulate inflammation following SCI and their involvement in neuronal regulation, offering potential targets and theoretical foundations for the diagnosis and treatment of SCI.

Materials and methods

Download expression matrix data. The expression matrix for GSE96055 (40) was derived from the GEO database (https://www.geoncbi.nlm.nih.gov/). The age of rats used in the data set is ~12 weeks and the data set is based on GPL17021 platform analysis (40). Microglia were purified by flow cytometry fluorescence sorter (FACS) in non-injured CX3CR1+/eGFP mice and at 3 time points (3, 7 and 14 days) following moderate and severe SCI (40). Gene profiles were then compared (Fig. 1A).

Data preprocessing and identification of differentially expressed genes (DEGs). The expression matrix was subjected to batch effect elimination and batch normalization using R software (v4.1.3; https://www.r-project.org/) and R-package SVA (v3.3; https://www.bioconductor.org/packages/release/bioc/html/sva.html) (41). The Limma package (v3.4; http://www.bioconductor.org/packages/release/bioc/html/limma.html) was used to identify DEGs by comparing expression values between the sham and SCI group (42). The adjusted $P<0.05$ and $|logFC|>1$ were used as the selection criteria (42).

Weighted correlation network analysis (WGCNA) and Random forest analysis (RF). WGCNA (v1.6.1; cran.r-project.org/web/packages/WGCNA/index.html) is a tool (43) for constructing gene co-expression networks and identifying gene clusters or modules, which was used to analyze highly relevant native gene clusters or modules for SCI. Based on the conventional gene screening method of WGCNA (44), the following parameters were set in the present study: A total of ≥10 cut-off genes, cutting height=0.90, Z-score ≥5 and stability-related stability correlation $P\leq0.05$; the connection of nodes (genes) between the two was used to calculate the dataset and genes with the correlation coefficient <0.5 were excluded. The conservation status of the WGCNA module and the traits-related characteristics were analyzed. RF (v4.7.1; https://www.bioconductor.org/packages/release/bioc/html/randomForest.html) is an integrated algorithm composed of decision trees and one of the commonly used machine learning algorithms (45). It can be used for both classification problems and regression problems (45). This algorithm was used to screen genes with variable importance >0 for subsequent analysis.

Functional enrichment analysis and protein-protein interaction network (PPI) analysis. Gene Set Enrichment Analysis (GSEA) (46) is a computational method that determines whether an a priori defined set of genes shows statistically significant, concordant differences between two biological states and its R package is clusterProfiler (47) (v4.0.5; https://www.bioconductor.org/packages/release/bioc/html/clusterProfiler.html). The Kyoto Encyclopedia of Genes and Genomes (KEGG), Gene Ontology (GO) and protein-protein interaction network (PPI) analysis was performed using the Metascape website (http://www.metascape.org/) (48). The connectivity (degree) and hub nodes (genes) in PPI (49) were obtained using scale-free property (48). The results of PPI were imported into

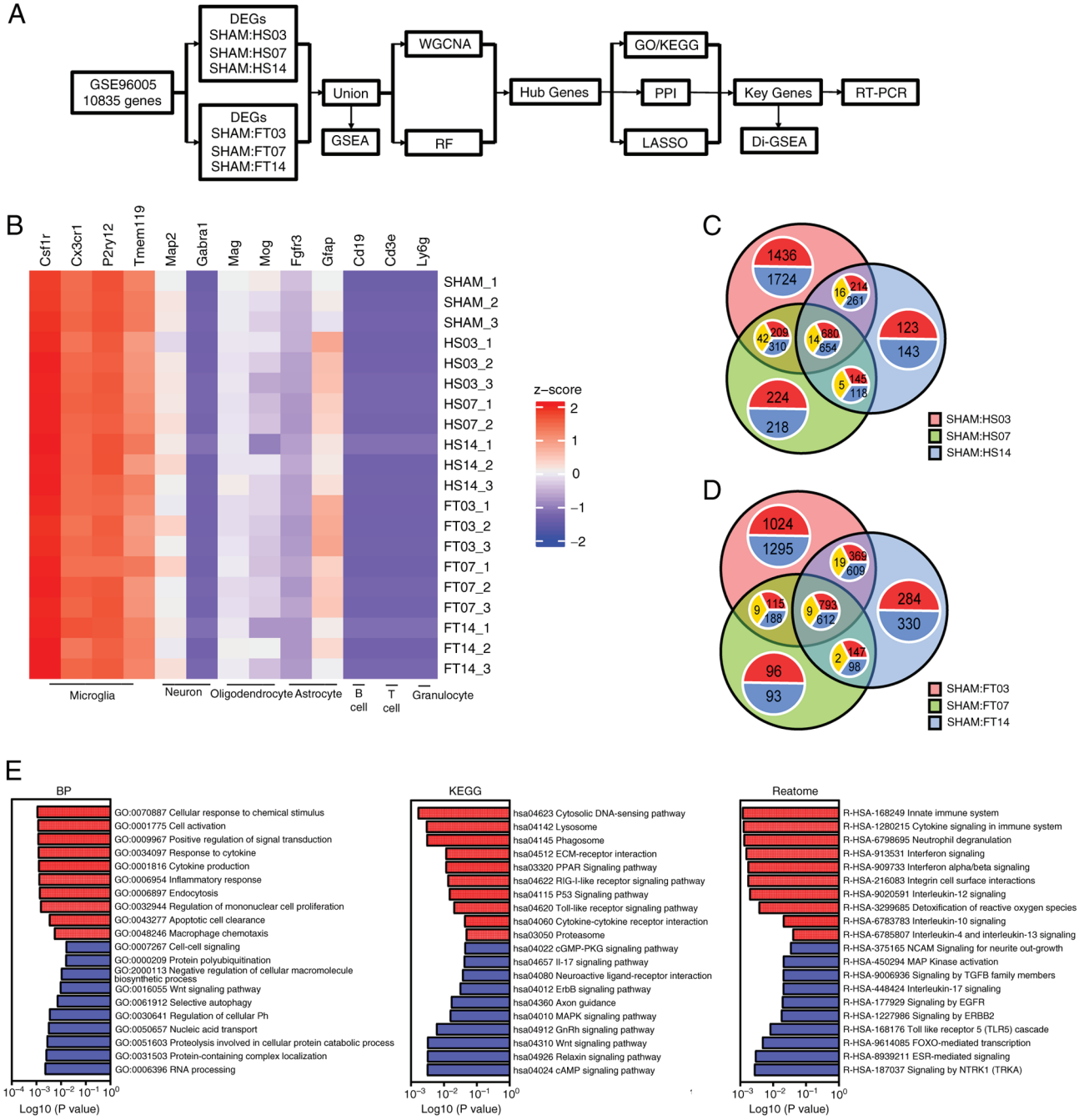

Figure 1. Identification of DEGs. (A) Research roadmap. (B) Heat map of relative expression levels of various cellular markers for 20 samples in the data set, with the deepest blue representing 0. Venn diagram of DEGs between the SHAM operation group and at 3, 7 and 14 days after SCI of the (C) HS and the (D) FT, respectively. In each annotation circle, red represented the number of upregulated genes, blue represented the number of downregulated genes and yellow represented the number of genes with the opposite trend in the intersection set. (E) BP, KEGG and Reactome analysis in GSEA between the SHAM and the SCI group. DEGs, differentially expressed genes; SCI, spinal cord injury; HS, hemiparaplegia injury group; FT, complete paraplegia injury group; BP, biological process; KEGG, Kyoto Encyclopedia of Genes and Genomes; GSEA, Gene Set Enrichment Analysis; WGCNA, weighted correlation network analysis; RF, random forest; PPI, protein-protein interaction network; RT-PCR, reverse transcription-quantitative PCR.

Cytoscape software (v3.9.1; http://www.cytoscape.org/) and further analyzed in combination with the results of DEGs.

Comparison of expression of hub genes. The heat map was generated using R-packages Complex-Heatmap (v3.1; https://cran.r-project.org/web/packages/ComplexHeatmap/index.html) and GGplots (v3.0; https://cran.r-project.org/web/packages/ggplots/index.html) to compare the expression levels of hub genes (50). The least absolute shrinkage and selection operator (LASSO) analysis (51) (v4.1.4; https://cran.r-project.org/web/packages/glmnet/index.html) is also one of the commonly used machine learning algorithms, which is characterized by variable selection and regularization while fitting the generalized linear model. The degree of adjustment of the regression complexity of LASSO is controlled by the parameter λ (51). The larger λ is, the stronger the penalization for the linear model with more variables (51). The goal is to choose the λ model corresponding

Table I. Gene primers used in the present study.

Gene	Name	Forward primer 5'-	Reverse primer 3'-
GAPDH	Glyceraldehyde-3-Phosphate Dehydrogenase	ACAGCAACAGGGTGGTGGAC	TTTGAGGGTGCAGCGAACTT
IL1b	Interleukin 1 β	GCCAGTGAAATGATGGCTTATT	AGGAGCACTTCATCTGTTTAGG
IL6	Interleukin 6	CACTGGTCTTTTGGAGTTTGAG	GGACTTTTGTACTCATCTGCAC
TNFα	Tumor necrosis factor α	AAGGACACCATGAGCACTGAAAGC	AGGAAGGAGAAGAGGCTGAGGAAC
Anxa2	Annexin A2	CTGGGGACTGACGAGGACT	GTTGATCTCTTGCAGCTCCTG
Myo1e	Myosin IE	AGAGCAAAGTCAACCCTCCTG	GGTTCCAGCTGTTGAAGTGC
Spp1	Secreted phosphoprotein 1	AGCTGGATGAACCAAGTCTGG	GGCTGTGAAACTTGTGGCTC

to the minimum variable characteristics and errors as much as possible because after the λ value reaches a certain size, continuing to increase the number of model-independent variables or reducing the λ value cannot significantly improve the model performance. Thus, a model with fewer variables is obtained finally. The present study calculated LASSO-Cox coefficients using a Lasso regression model to select key genes in microglia following SCI.

Cell culture and reverse transcription-quantitative (RT-q) PCR. The microglia cell line BV2 was purchased from the China Academy of Sciences Cell Bank. LPS can stimulate microglia to switch to M1 phenotype to express pro-inflammatory cytokines (52). The present study used LPS to simulate the neuroinflammatory state. The relative expression levels of the common pro-inflammatory factors IL1b, IL6 and TNF were measured to verify whether the BV2 cells were converted to M1 type. Following resuscitation of BV2 microglia, 10% fetal bovine serum (cat. no. 30067334; Invitrogen; Thermo Fisher Scientific, Inc.) was added into DMEM medium (cat. no. 11320033; Invitrogen; Thermo Fisher Scientific, Inc.) and incubated at 37˚C and 5% CO_2 for at least 8 h. The medium was changed every other day and passaged every 2 days. The morphology of the cells was observed under a light microscope at a magnification of x20. After the BV2 microglia entered the logarithmic phase, the cells were stimulated with LPS (100 ng/ml) for 6, 12 and 24 h. Total RNA was isolated using TRIzol® reagent (Thermo Fisher Scientific, Inc.) and reverse transcribed into cDNA according to the manufacturer's instructions. TRIzol® (500 μl) was added and mixed well. A total of 200 μl chloroform was added, shaken and allowed to stand for 5 min. The mixture was centrifuged at 4˚C, 4,000 x g for 15 min and collected the upper phase. An equal amount of isoamyl alcohol was added, mixed evenly and allowed to stand for 5 min. After centrifuging at 4˚C, 4,000 g for 10 min, the supernatant was discarded. 1 ml of 75% ethanol was added with gentle oscillation. The RNA concentration was determined after drying. The cell density for RNA extraction is approximately $8x10^5$/ml, and RNA purity and quantification are tested by spectrophotometry. RNA extraction, cDNA synthesis, and qPCR are performed according to the manufacturer's protocol. RT-qPCR was performed using SYBR green dye (Takara Biotechnology Co., Ltd.) under the following parameters: Initial denaturation step at 95˚C for 30 min; 40 cycles at 95˚C for 5 sec; and 60˚C for 30 sec. Each sample was repeated three times independently and the PCR results were statistically analyzed by the $2^{-\Delta\Delta Cq}$ method (53). The entire experimental procedure was completed independently for each sample. The mRNA primers are shown in Table I.

ELISA. The expression levels of Anxa2 (cat. no. E1944r; ElAab Biotechnology Inc.), Myo1e (cat. no. KTE61422; Abbkine Scientific Co., Ltd.) and Spp1 (cat. no. E0899m; ElAab Biotechnology, Inc.) in BV2 cells were determined by ELISA kits. The sample were stored at -80˚C before measurement. The optical density at 450 nm was calculated by subtracting the background value and the standard curve was drawn.

Data analysis. SPSS 22.0 software (IBM Corp.) was used for all statistical analyses. One-way ANOVA was used for comparison between groups. All experiments were independently repeated three times. Tukey's honestly significant difference test was conducted as post-hoc analyses. All data are presented as the mean ± SEM. GraphPad Prism 6 (Dotmatics) was used for plotting. $P<0.05$ was considered to indicate a statistically significant difference.

Results

Identification of DEGs. Following standardized pretreatment of microarray results from GSE96055, the present study compared the expression levels of microglia and other cell marker genes. The analysis revealed that the sequencing target in the dataset was microglia following SCI (Fig. 1B). DEGs were identified by comparing the SHAM group with the SCI group at 3, 7 and 14 days, leading to the detection of a total of 6,513 DEGs in the hemiparaplegia injury group as moderate SCI and 1,348 DEGs in the common intersection of the three groups (Fig. 1C). In comparison with the SHAM group, the 3-day group exhibited 1,724 downregulated genes and 1,436 upregulated genes, while the 7-day group showed 218 downregulated genes and 224 upregulated genes and the 14-day group displayed 143 downregulated genes and 123 upregulated genes (Fig. 1C). In the complete paraplegia injury group, as severe SCI, 6,076 DEGs were detected, with 1,414 DEGs at the intersections shared by the three groups (Fig. 1D). The SHAM group demonstrated 1,295 downregulated genes and 1,024 upregulated genes compared with the 3-day group, 93 downregulated genes and 96 upregulated genes compared with the 7-day group and 330 downregulated genes and

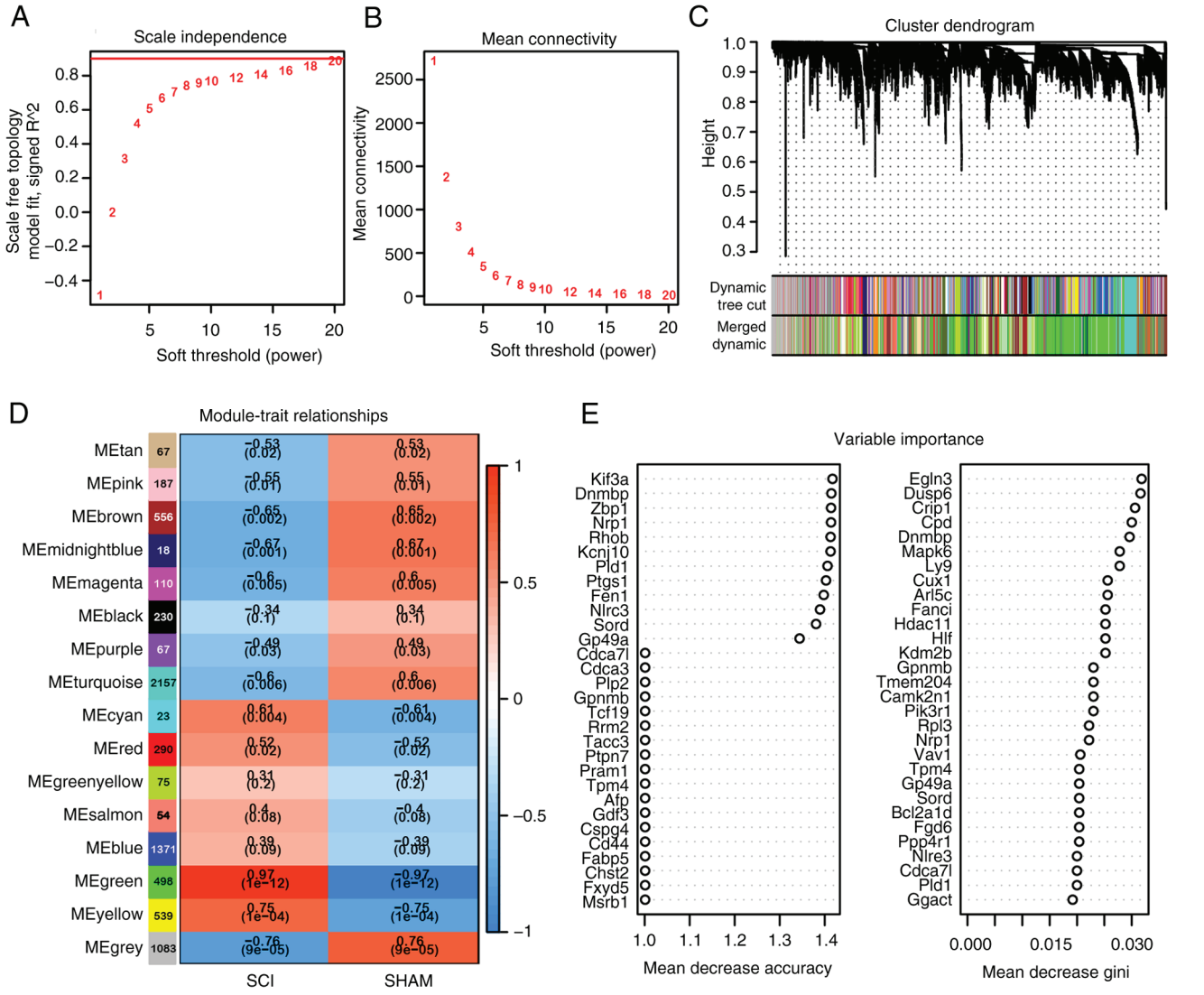

Figure 2. WGCNA and RF of DEGs. (A) Scale independence. (B) Mean connectivity. The network topology analysis for adjacency matrix with different soft threshold power. Red numbers in the boxes indicate the soft thresholding power corresponding to the correlation coefficient square value (y-axis). (C) Consensus module dendrogram was produced by 7,340 DEGs with a variation coefficient of expression >0.1, based on the criteria of correlation coefficient square of eigengenes above 0.90, soft threshold power of 18, the number of genes >10 and cut height=0.90. (D) Module-trait associations. Each row corresponds to a module trait gene and each column corresponds to a trait. Red indicated a positive correlation between modular trait genes and traits and blue indicated a negative correlation. Each cell contains correlation coefficient ρ and the P-value in parentheses. (E) Two calculation methods of DEGs related to SCI for random forest screening. Mean decrease accuracy: The reducing degree of the accuracy of the random forest prediction by changing the value of a variable into a random number. A larger value indicates that the variable is more significant. Mean decrease gini: The effect of each variable on that heterogeneity of the observation at each node of the classification tree is calculated to compare the importance of the variable. A larger value indicates that the variable is more significant. WGCNA, weighted correlation network analysis; RF, random forest; DEGs, differentially expressed genes; SCI, spinal cord injury.

284 upregulated genes compared with the 14-day group (Fig. 1D). Altogether, 7,340 DEGs were identified across both groups with varying degrees of SCI. GSEA performed on these genes indicated their close association with the progression of neuroinflammation, highlighting enhanced recruitment of microglia, heightened endocytosis and intensified inflammatory responses, along with increased expression levels of various inflammatory cytokine signaling pathways (Fig. 1E).

WGCNA and RF analysis of DEGs. The expression matrix of 7,340 DEGs was used for network construction. A soft threshold power of 18 was determined for the adjacency matrix and module recognition in WGCNA was carried out based on a gene correlation coefficient >0.90 (Fig. 2A). The resulting gene modules demonstrated a near scale-free topology standard (Fig. 2B). After determining the soft threshold, the expression matrix of differential genes was further processed to identify modules using hierarchical clustering and the dynamic cutting algorithm (Fig. 2C). A total of 15 different co-expression modules were identified and visualized in different colors, with the Green module displaying the highest correlation coefficient with SCI (ρ=0.97) and the smallest P value ($P=10^{-12}$), indicating strong association with subacute SCI (Fig. 2D). This module comprised 498 genes. Subsequently, RF analysis was conducted on the 7,340 DEGs to select genes highly relevant to microglia following SCI, resulting in the identification of 458 genes (Fig. 2E).

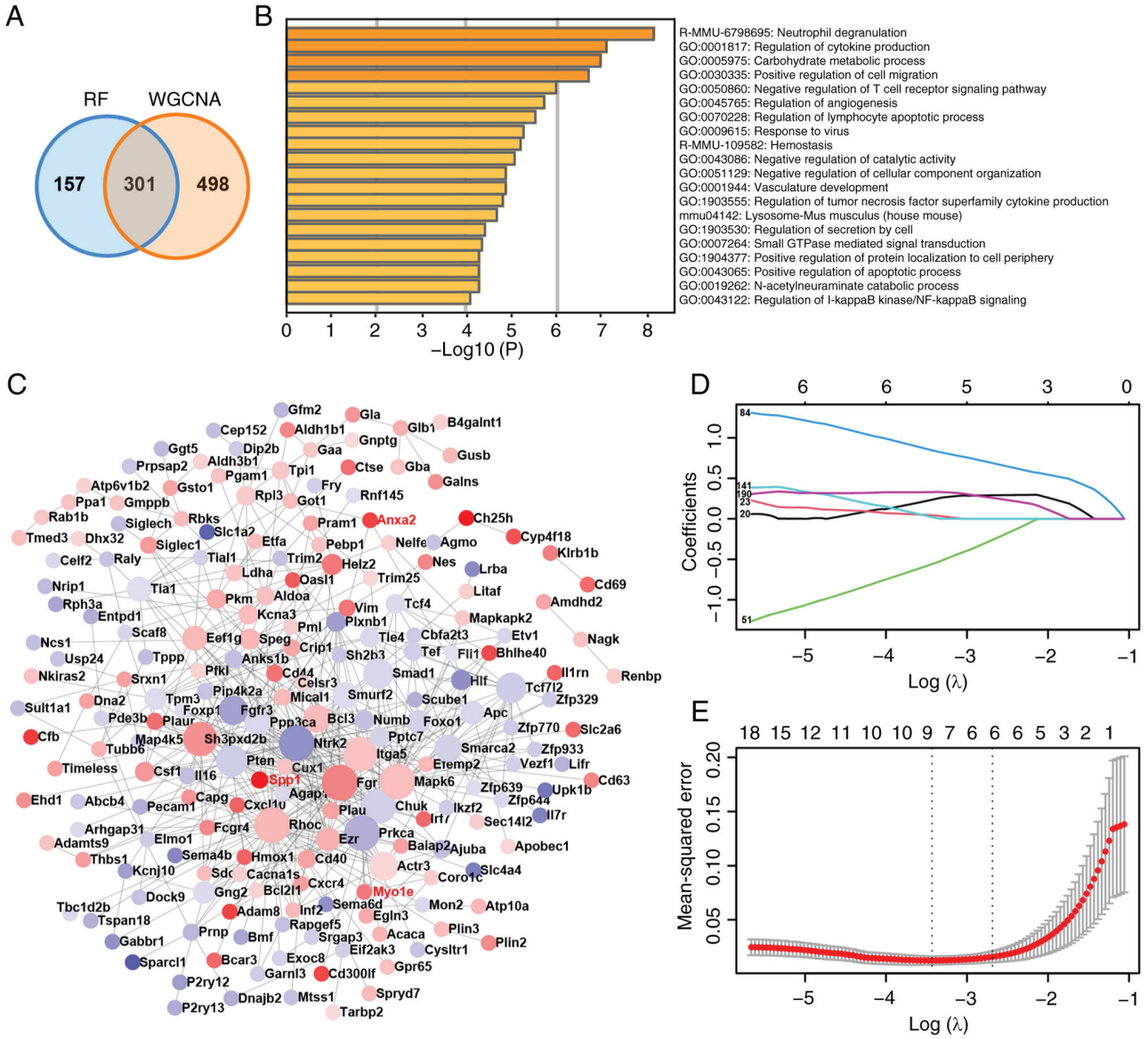

Figure 3. Functional enrichment, PPI and LASSO analysis of hub genes. (A) Venn diagram of intersection genes between WGCNA and RF. (B) Functional enrichment analysis for 301 hub genes. (C) PPI analysis of hub genes. Red indicates that the gene expression level is upregulated after SCI and blue indicates that the gene expression level is downregulated. The darker the color, the greater the difference in expression level. (D) The locus of change of independent variable coefficient of LASSO analysis. Each curve in the figure represents the change trace of coefficient of each independent variable. The ordinate is the value of the coefficient, the lower abscissa is log(λ) and the upper abscissa is the number of non-zero coefficients in the model at this time. The later the coefficient is compressed to 0, the more important the variable is as the value of λ changes. (E) Model error diagram of LASSO analysis. On the ordinate is Mean-Squared Error. Cross Validation of LASSO analysis allows that for each λ value, around the mean of the target parameter shown by the red dot, one can obtain the confidence interval of the target parameter. There are two numerical dashed lines, the line with the lowest error on the left (λmin) and the line with the least feature on the right (λ1se), which are 0.03236614 and 0.0763 respectively. λmin is the average of the minimum objective parameters that give all λ values. The value of λ1se is a model with good performance but the least parameters. When λ1se was chosen, the performance of the model is the best. PPI, protein-protein interaction; LASSO, least absolute shrinkage and selection operator; WGCNA, weighted correlation network analysis; RF, random forest; SCI, spinal cord injury; PPI, protein-protein interaction network; GO, Gene Ontology.

Functional enrichment, PPI and LASSO of hub genes. The intersection of 498 genes in the green module of WGCNA and 458 genes in RF yielded 301 hub genes (Fig. 3A). Further analysis of the GO functions and KEGG pathways of these hub genes suggested a close association between post-SCI microglia and neuroinflammation, participating in the regulation of apoptosis (Fig. 3B and Table II). PPI revealed that 205 genes could serve as central nodes, with the expression levels of 111 genes upregulated and 94 genes downregulated post-SCI (Fig. 3C). Subsequently, through LASSO analysis of the 205 hub nodes (Fig. 3D and E), key genes were identified. The two dashed lines in Fig. 3E represent two specific λ values, namely λmin and λ1se, which were 0.03236614 and 0.0763, respectively. λ-min is the average minimum targeted parameter value of all λ values. The λ1se value represents a model with good performance and minimal parameters. When selecting λ1se, the performance of the model is optimal. Ultimately, the top three key genes in LASSO based on parameter values were identified as Anxa2, Myo1e and Spp1.

Single-gene GSEA analysis of key genes. To further investigate the specific functional mechanisms of these three key

Table II. Top 20 results of the GO function and KEGG pathway of 301 hub genes.

Category	GO	Description	PARENT_GO	Genes	LogP-value	Enrichment
Reactome gene sets	R-MMU-6798695	Neutrophil degranulation	-	Adam8 Aldoa Glb1 Anxa2 Cd44 Cd63 Fgr Gaa Lilrb4b Lilrb4a Clec4d Pecam1 Pfkl Pgam1 Pkm Plau Plaur Syngr1 Galns Aldh3b1 Bst2 Glipr1 Qsox1 Olr1 Cyb5r3 Gusb Fcgr4	-8.24468	3.7055244
GO Biological processes	GO:0001817	Regulation of cytokine production	19_GO:0032501 multicellular organsmal process	Adam8 Bcl3 Tspo Chuk Eif2ak3 Fgr Gba Lilrb4b Lilrb4a Hmox1 Il16 Mapkapk2 Cd244a Pml Prnp Thbs1 Tia1 Cd40 Tnfsf9 Ezr Clec4a2 Tlr5 Irf7 Litaf Bst2 Sulf2 Foxp1 Cgas Cd300ld Oas2 Nlrc3 Akirin2	-7.18245	2.9129408
GO Biological processes	GO:0005975	Carbohydrate metabolic process	19_GO:0008152 metabolic process	Gla Aldoa Glb1 Gaa Ggta1 Got1 Gsto1 Ldha Pfkl Pgam1 Pkm Pten Renbp Tcf7l2 Tpi1 Chst7 Rbks Gusb Kbtbd2 Pgghg Slc39a14 Gnptg Amdhd2	-7.03583	3.6779535
GO biological processes	GO:0030335	Positive regulation of cell migration	19_GO:0040011 locomotion	Adam8 Aldoa Apc Rhoc Cxcr4 Csf1 Fgr Gcnt2 Hmox1 Cxcl10 Itga5 Lgals3 Numb Pecam1 Prkca Plau Ppp3ca Sema4b Thbs1 Cd40 Elp5 Smurf2 P2ry12 Actr3 Foxp1 Sema6d	-6.74981	3.2225668
GO biological processes	GO:0050860	Negative regulation of T cell receptor signaling pathway	19_GO:0002376 immune system process	Lilrb4b Lilrb4a Lgals3 Prnp Ezr Dgkz	-6.00218	17.193633
GO Biological processes	GO:0045765	Regulation of angiogenesis	19_GO:0032502 developmental process	Cxcr4 Hmox1 Cxcl10 Itga5 Lgals3 Sh2b3 Smad1 Pde3b Pkm Prkca Pml Tcf4 Thbs1 Cd40 Cysltr1 Ecscr Adamts9	-5.76361	3.9541635
GO Biological processes	GO:0070228	Regulation of lymphocyte apoptotic process	19_GO:0050789 regulation of biological process	Adam8 Bcl3 Cd44 Il7r Lgals3 Pten Siglec1 Prelid1 Foxp1	-5.53873	7.5854264
GO Biological processes	GO:0009615	Response to virus	19_GO:0044419 biological process involved in inter-species interaction between organisms	Apobec1 Bcl2l1 Bcl3 Chuk Cxcl10 Pml Cd40 Serinc3 Irf7 Zmynd11 Bst2 Ifi27l2a Cgas Trim25 Oasl1 Oas2	-5.2859	3.833586
Reactome gene sets	R-MMU-109582	Hemostasis	-	Aldoa Anxa2 Cd44 Cd63 Ehd1 Fgr Gng2 Itga5 Sh2b3 Cd244a Pecam1 Prkca Plau Plaur Scg3 Sdc3 Tubb6 P2ry12 Qsox1 Dgkz Olr1	-5.2376	3.0765704
GO biological processes	GO:0043086	Negative regulation of catalytic activity	19_GO:0065007 biological regulation	Gla Apc Cd44 Gba Lilrb4b Lilrb4a Ajuba Sh2b3 Nes Pecam1 Pip4k2a Prkca Plaur Pml Prnp Pten Renbp Thbs1 Coro1c Pebp1 Gabbr1 Camk2n1 P2ry13 Mical1 Slc39a14	-5.10305	2.6891944

Table II. Continued.

Category	GO	Description	PARENT_GO	Genes	LogP-value	Enrichment
GO Biological processes	GO:0051129	Negative regulation of cellular component organization	19_GO:0048519 negative regulation of biological process	Apc Apobec1 Bcl2l1 Tspo Capg Ch25h Fgfr3 Gba Cxcl10 Lgals3 Nrxn1 Pecam1 Pml Ppp3ca Prnp Pten Sema4b Vim Coro1c Dnajb2 Prelid1 Actr3 Scaf8 Sema6d Dip2b Nlrc3	-4.94884	2.5727122
GO Biological processes	GO:0001944	Vasculature development	19_GO:0032502 developmental process	Adam8 Anxa2 Cxcr4 Eif2ak3 Hmox1 Itga5 Nrxn1 Ntrk2 Pde3b Pecam1 Prkca Plau Pten Tcf7l2 Thbs1 Vezf1 Foxo1 Efemp2 Smarca2 Ecscr Myo1e Adamts9 Tmem204	-4.9376	2.7692827
GO Biological processes	GO:1903555	Regulation of tumor necrosis factor superfamily cytokine production	19_GO:0032501 multicellular organismal process	Adam8 Bcl3 Tspo Lilrb4b Lilrb4a Mapkapk2 Thbs1 Clec4a2 Foxp1 Cd300ld Oas2 Nlrc3	-4.83124	4.5485802
KEGG Pathway	mmu04142	Lysosome-Mus musculus (house mouse)	-	Gla Glb1 Cd63 Ctse Gaa Gba Galns Litaf Gusb Gnptg	-4.69035	5.3066769
GO biological processes	GO:1903530	Regulation of secretion by cell	19_GO:0051179 localization	Bcl2l1 Tspo Anxa2 Entpd1 Fgr Ncs1 Hmox1 Il1rn Lgals3 Ntrk2 Pde3b Pfkl Prkca Ppp3ca Rph3a Spp1 Tcf7l2 Ezr Gabbr1 Camk2n1 P2ry12 Mical1 Rhbdf2 Pram1	-4.43565	2.5100194
GO biological processes	GO:0007264	Small GTPase ediated signal transduction	19_GO:0023052 signaling	Rhoc Arhgap31 Chuk Csf1 Hmox1 Pecam1 Bcar3 Nkiras2 Dgkz Dock9 Baiap2 Elmo1 Rapgef5	-4.34358	3.785861
GO Biological processes	GO:1904377	Positive regulation of protein localization to cell periphery	19_GO:0051179 localization	Lgals3 Nrxn1 Prnp Ezr Actr3 Efcab7 Atp2c1	-4.30585	7.2678401
GO Biological processes	GO:0043065	Positive regulation of apoptotic process	19_GO:0048518 positive regulation of biological process	Adam8 Apc Bcl2l1 Tspo Cd44 Eif2ak3 Fgfr3 Hmox1 Ldha Pml Prnp Pten Siglec1 Tcf7l2 Thbs1 Tia1 Cd40 Serinc3 Foxo1 Prelid1 Ecscr Bmf	-4.32452	2.5965124
GO biological processes	GO:0019262	N-acetylneuraminate catabolic process	19_GO:0008152 metabolic process	Renbp Nagk Amdhd2	-4.28246	35.820069
GO Biological processes	GO:0043122	regulation of I-κB inase/NF-κB signaling	19_GO:0023052 signaling	Chuk Lilrb4b Lilrb4a Ajuba Clec4d Cd40 Zmynd11 Nkiras2 Trim25 Card6 Nlrc3	-4.09049	4.1258718

GO, Gene Ontology; KEGG, Kyoto Encyclopedia of Genes and Genomes.

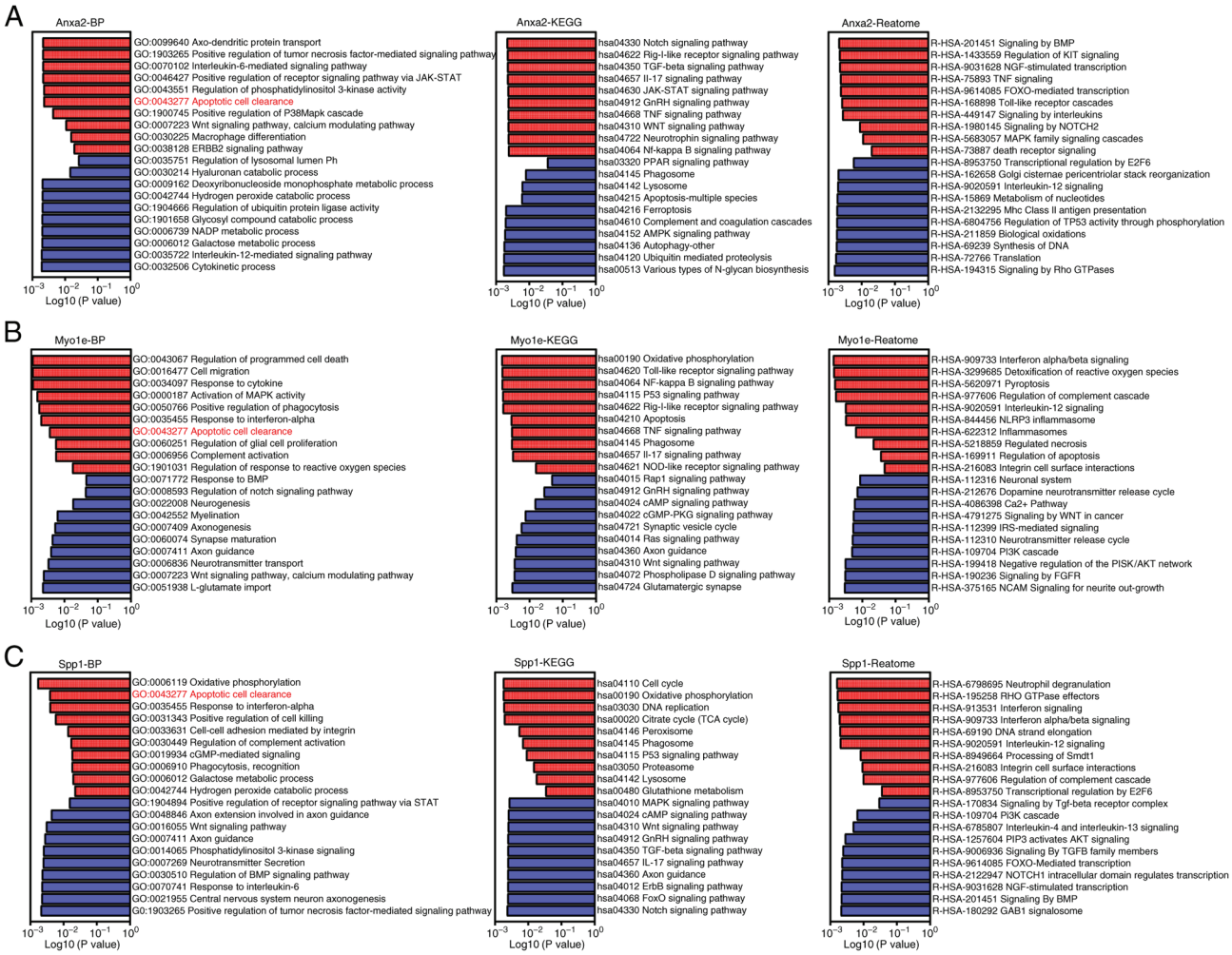

Figure 4. Single-gene GSEA analysis of key genes. BP, KEGG and Reactome analysis in GSEA analysis between the high-expression and low-expression group of (A) Anxa2. (B) Myo1e. (C) Spp1. BP, biological process; KEGG, Kyoto Encyclopedia of Genes and Genomes; GSEA, Gene Set Enrichment Analysis.

genes, single gene GSEA analysis was conducted, dividing 20 samples into corresponding high and low expression groups based on the expression levels of Anxa2, Myo1e and Spp1. The results showed a close correlation between the upregulation of Anxa2 in post-SCI microglia and inflammatory factors such as IL-6, IL-17 and TNF signaling pathways (Fig. 4A). Similarly, activation of JAK-STAT, p38MAPK cascade and Notch signaling pathways was observed (Fig. 4A). In addition, Myo1e was upregulated in post-SCI microglia and may participate in mechanisms such as enhanced responsiveness to interferons, increased expression of inflammatory signaling pathways and NF-κB activation (Fig. 4B). Spp1 was closely associated with enhanced phagocytic activity and complement activation in post-SCI microglia (Fig. 4C). Notably, in the biological functional analysis of these three genes, all three key genes were closely related to the gene set involved in the clearance of apoptotic cells, suggesting that these key genes may play important roles in the mechanism of clearing apoptotic cells in post-SCI microglia (Fig. 4A-C).

Comparison and verification of expression of key genes. The present study analyzed the relative expression levels of three key genes from the GSE96055 dataset to study their expression patterns in post-SCI microglia, considering changes in time and severity of injury (Fig. 5A-C). The expression levels of Anxa2 and Spp1 appeared to be minimally affected by injury time and severity, while the expression level of Myo1e slightly increased with time post-injury. In addition, the expression levels of 203 central genes in the dataset were examined and a heatmap generated (Fig. 5D). Heatmap analysis revealed that genes with upregulated expression in the upper part were more influenced by the injury time than the severity, whereas genes in the lower part exhibited the opposite trend (Fig. 5D).

It is known that the phagocytic cell receptor MerTK regulates phagocytic activity in BV2 cells (54). To determine whether key genes are involved in the clearance of apoptotic cells in BV2 cells, cells were treated with LPS (100 nM) and the MerTK-specific inhibitor UNC569 (500 nM) and changes in gene expression monitored. Compared with the control group, Anxa2, Myo1e and Spp1 mRNA levels were upregulated in the LPS group, indicating increased expression in pro-inflammatory microglial states, while they were downregulated in the LPS + UNC569 group, suggesting that inhibition of phagocytosis also suppressed their expression (Fig. 6A-C). Consistent with mRNA results, protein levels of Anxa2, Myo1e and Spp1 exhibited a similar trend (Fig. 6D-F).

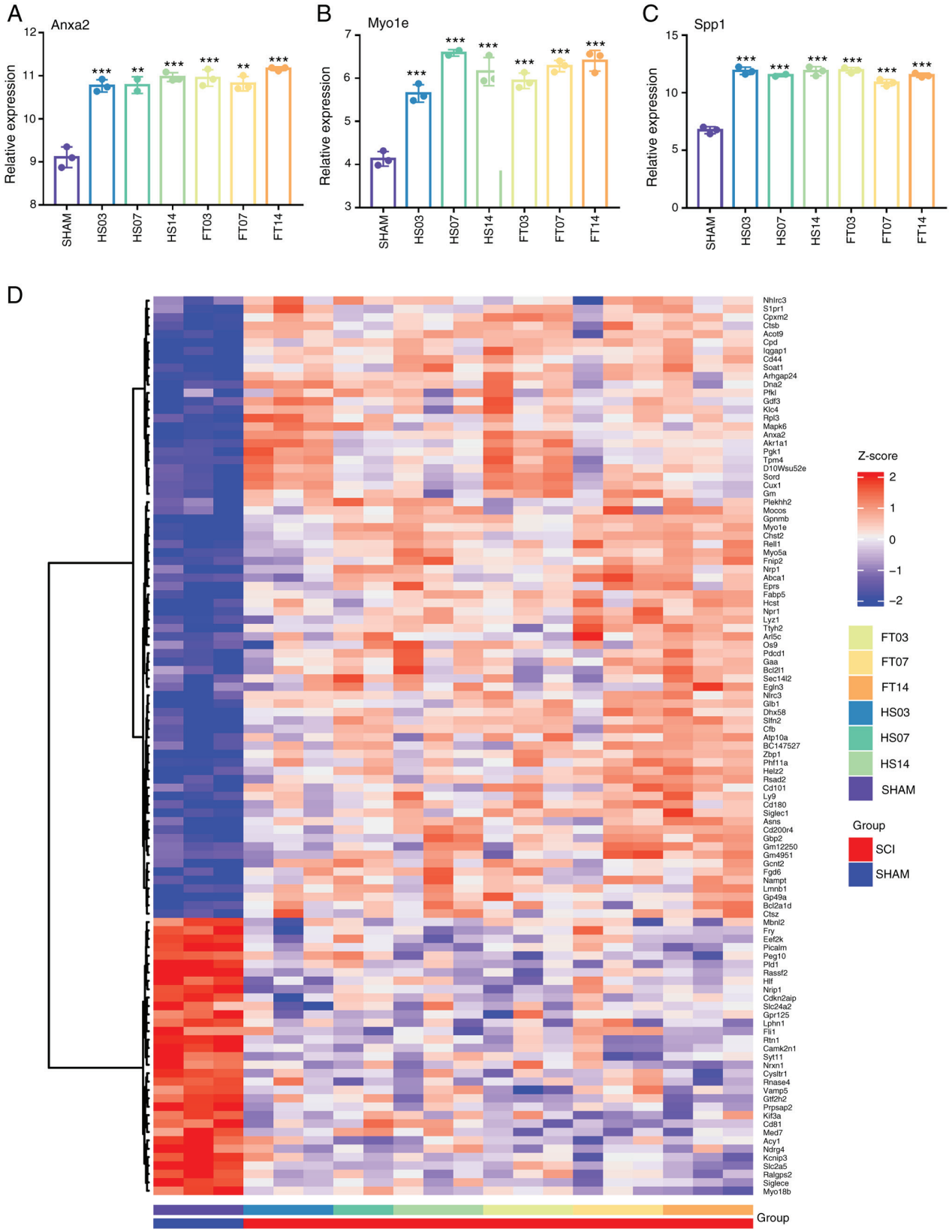

Figure 5. Comparison of hub genes expression levels. Histogram of relative expression levels of (A) Anxa2, (B) Myo1e and (C) Spp1 in GSE96055 expression matrix. (D) Heat map of 203 hub nodes in PPI. PPI, protein-protein interaction. **P<0.01, ***P<0.001 vs. sham.

Discussion

In the present study, through bioinformatics analysis, a close correlation was discovered between microglia after SCI and neuroinflammation and efferocytosis. It is worth noting that the expression levels of Anxa2, Myo1e and Spp1 in microglia following SCI were significantly upregulated. These three genes are closely associated with various biological functions,

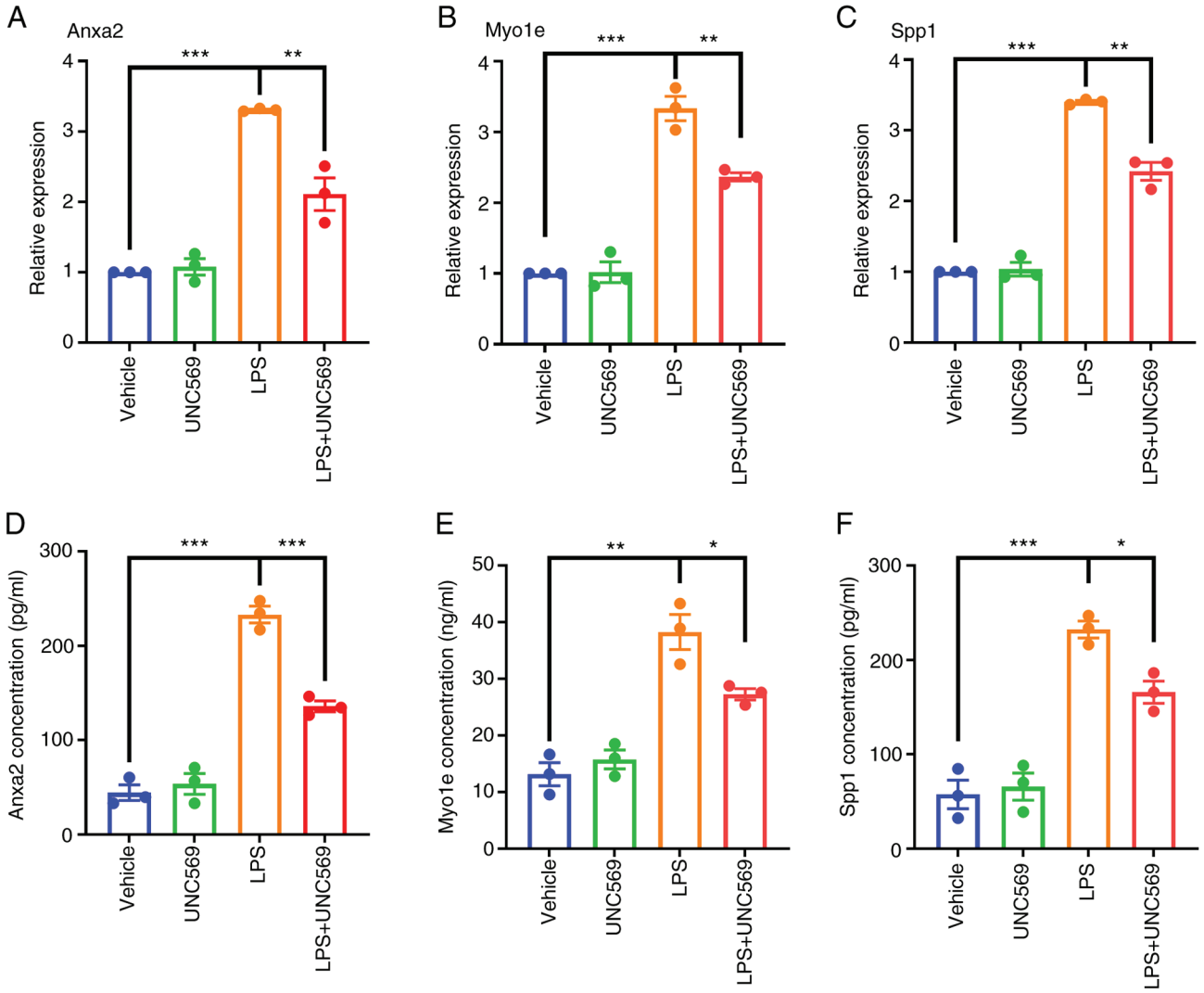

Figure 6. RT-qPCR and ELISA validation. The mRNA expression levels of (A) Anxa2, (B) Myo1e and (C) Spp1. (The protein expression levels of three key genes, (D) Anxa2, (E) Myo1e and (F) Spp1. A total of three samples per group in duplicate were summarized as the mean ± SEM with P<0.05. BV2 microglia were stimulated with 100 ng/ml LPS for 6, 12 and 24 h, compared with the unstimulated group, respectively. One-way ANOVA was performed. *P<0.05, **P<0.01, ***P<0.001. RT-qPCR, reverse transcription-quantitative PCR; SCI, spinal cord injury; SE, standard error; LPS, lipopolysaccharide.

such as signaling pathways involved in the release of inflammatory factors, amplification of inflammatory cascades and phagocytosis. Notably, they are all significantly enriched in the gene set related to the clearance of apoptotic cells.

GSEA results for the SHAM group and SCI group revealed that microglia mainly play an immunomodulatory role and participate in the polarization and recruitment of macrophages derived from microglia and monocytes at the site of injury. Additionally, they regulate the secretion of interleukins and interferons. These results indicated that microglia primarily play a pro-inflammatory role at the site of SCI, consistent with the views of other researchers (12-14). Widely used machine learning algorithms, WGCNA, RF and LASSO analysis, have been employed in biomedical research, typically used individually (55,56). The present study integrated these three different algorithms for key gene screening and analysis for the first time, to the best of the authors' knowledge. WGCNA focuses on specific phenotypes and co-expression modules, where genes within the same module are considered functionally related with higher reliability and biological significance (56). RF evaluates the importance of variables in determining categories (57,58), while LASSO effectively selects features and addresses multicollinearity issues (59).

Conventional bioinformatics analysis relies on researchers manually designing rules and processes, which introduces subjectivity and limitations, potentially hindering the full exploration of potential patterns and information within the data, as well as struggling to effectively handle complex data structures and relationships. The present study effectively identified and predicted biological characteristics, gene expression patterns and disease-related genes of microglial cells post-SCI using the GSE96055 dataset for machine learning algorithms, thereby enhancing the accuracy and precision of data analysis. It identified a characteristic gene set of microglia after SCI and found that key genes Anxa2, Myo1e and Spp1 are closely associated with the clearance of apoptotic cells.

The clearance of apoptotic cells is crucial for the restoration of extracellular environment homeostasis (60). Despite extensive attention to efferocytosis in inflammatory macrophages (61) and cancerous macrophages (62), specific research

on the mechanisms of microglia in the nervous system, particularly after SCI, is lacking. The MerTK signaling pathway plays a vital role in the clearance of apoptotic cells by microglia (63). In the present study, the MerTK-specific inhibitor UNC569 was used to suppress the clearance of apoptotic cells in microglia, widely utilized for the phagocytic clearance function of microglia (54). Finally, the results of analysis were validated using BV2 cells *in vitro*, consistent with the findings of the bioinformatics analysis.

Anxa2, a member of the calcium-dependent phospholipid-binding protein family, plays a role in cell growth regulation and signal transduction pathways (64,65). Anxa2 is involved in various cellular processes such as proliferation, differentiation, apoptosis, migration, membrane repair, immune suppression and inflammatory responses, closely associated with the prognosis and severity of various diseases (66-68). GSEA analysis of Anxa2 suggested its involvement in regulating relevant inflammatory factor signaling pathways, consistent with the findings of other researchers. Previous studies have shown that Anxa2 promotes phagocytic cell assembly, regulates the endosomal recycling pathway and multicellular endosome biogenesis (69,70). Anxa1 has been implicated in the efferocytosis of microglia. In addition, GSEA analysis of Myo1e and Spp1 indicated their participation in regulating inflammation responses and inflammatory factor signaling pathways related to microglia. Myo1e, as an unconventional myosin, plays various critical roles in physiological processes such as cell adhesion, migration, phagocytosis and cell expulsion based on its motility and structural features (71,72). Spp1, a non-collagenous bone protein, has been shown to modulate macrophage polarization (73). Recent studies suggest a crucial role for Spp1 in monitoring and regulating acute and chronic neuroinflammation (74,75). Notably, SPP1 induces phagocytic and synaptic engulfment of microglia in an Alzheimer's disease mouse model (76).

These research findings are consistent with the discoveries of the present study. In the results of single-gene GSEA analysis, the three key genes Anxa2, Myo1e and Spp1 not only play a negative role in regulating inflammation but also actively participate in the clearance of apoptotic cells, which may be a critical manifestation of the dual role of microglia after SCI. However, there is a lack of literature on their specific roles in clearing apoptotic cells. The present study suggested that they may be involved in regulating efferocytosis mechanisms, serving as important targets for treating SCI. Whether these three key genes can be used as indicators to determine the progression of SCI requires extensive clinical research practice.

Despite significant progress in research on the clearance of apoptotic cells, the study of efferocytosis mechanisms in the CNS is still in its early stages. Combining results from studies of other diseases, the type of disease and the duration of the disease, efferocytosis may have different effects on disease progression (11). Studies have indicated significant differences in the phagocytic response of peripheral macrophages and microglia and variations in the efficiency of neuronal apoptosis clearance. Additionally, compared with brain injuries, the phagocytic capacity and phagocytic cell ratio of microglia after SCI are quite heterogeneous (77-79). There is a lack of literature on specific mechanisms, necessitating further research. In SCI, current research suggests that white matter and gray matter microglia have different transcriptional profiles in disease progression and spatial axes (7,10). However, their contributions to the clearance of apoptotic cells remain unk*n*own, highlighting the need for further investigation into the efferocytosis functions of microglia with different functional phenotypes and how to regulate microglia to exert neuroprotective effects.

However, the present study had some limitations. The data used for analysis came from experimental animal models, which may have limitations in the applicability of the analysis results to human disease models due to genomic differences between species. Subsequent studies should establish disease models using different animal species, compare the consistency and differences in various models and validate the results in human tissues to enhance the reliability and applicability of the findings. In addition, future research should integrate proteomic, single-cell sequencing and spatial transcriptomic data to comprehensively reflect the functional mechanisms of microglia post-SCI, providing clues to uncover the pathological mechanisms of SCI.

In conclusion, the present study showed that microglia after SCI play essential roles not only in neuroinflammation but also in the mechanism of apoptotic cell clearance. Notably, the expression levels of Anxa2, Myo1e and Spp1 in microglia after SCI are significantly upregulated, potentially participating in the regulation of apoptotic cell clearance mechanisms. The present study suggested that Anxa2, Myo1e and Spp1 may be potential targets for future SCI treatments, providing a scientific basis for the development of new therapeutic approaches and drugs for SCI.

Acknowledgements

Not applicable.

Funding

The present study was supported by the Project of Nantong Municipal Health Commission (grant no. MS2022016), the Project of Nantong First People's Hospital (grant no. YPYJJZD008), the Postgraduate Research & Practice Innovation Program of Jiangsu Province (grant no. KYCX21_3107), Project of Jiangsu Administration of Traditional Chinese Medicine (grant no. MS2022090), the General Project of Nantong Basic Scientific Research (grant no. JC22022067), The Scientific Research Innovation Team Project of Nanjing Medical University Kangda College (grant no. KD2022KYCXTD011) and the special key project of clinical basic research in Nantong University (grant no. 2022JZ004).

Availability of data and materials

The data generated in the present study may be requested from the corresponding author.

Authors' contributions

LY conceived and designed the experiments, analyzed the data and prepared figures and/or tables. Data collections were

performed by LLW, CC, JYH, GHX, JWJ, JJC, CSW and HXH. ZMC contributed to the study conception and design. The first draft of the manuscript was written by LY and all authors commented on previous versions of the manuscript. LY and ZMC confirm the authenticity of all the raw data. All authors read and approved the final manuscript.

Ethics approval and consent to participate

Not applicable.

Patient consent for publication

Not applicable.

Competing interests

The authors declare that they have no competing interests.

References

1. Anjum A, Yazid MD, Daud MF, Idris J, Ng AMH, Naicker AS, Ismail OHR, Kumar RK and Lokanathan Y: Spinal cord injury: Pathophysiology, multimolecular interactions, and underlying recovery mechanisms. Int J Mol Sci 21: 7533, 2020.
2. Hu X, Xu W, Ren Y, Wang Z, He X, Huang R, Ma B, Zhao J, Zhu R and Cheng L: Spinal cord injury: Molecular mechanisms and therapeutic interventions. Signal Transduct Target Ther 8: 245, 2023.
3. Calvert JS, Grahn PJ, Zhao KD and Lee KH: Emergence of epidural electrical stimulation to facilitate sensorimotor network functionality after spinal cord injury. Neuromodulation 22: 244-252, 2019.
4. Thomaz SR, Cipriano G Jr, Formiga MF, Fachin-Martins E, Cipriano GFB, Martins WR and Cahalin LP: Effect of electrical stimulation on muscle atrophy and spasticity in patients with spinal cord injury-a systematic review with meta-analysis. Spinal Cord 57: 258-266, 2019.
5. Brockie S, Hong J and Fehlings MG: The role of microglia in modulating neuroinflammation after spinal cord injury. Int J Mol Sci 22: 9706, 2021.
6. Nimmerjahn A, Kirchhoff F and Helmchen F: Resting microglial cells are highly dynamic surveillants of brain parenchyma in vivo. Science 308: 1314-1318, 2005.
7. van der Poel M, Ulas T, Mizee MR, Hsiao CC, Miedema SSM, Adelia, Schuurman KG, Helder B, Tas SW, Schultze JL, *et al*: Transcriptional profiling of human microglia reveals grey-white matter heterogeneity and multiple sclerosis-associated changes. Nat Commun 10: 1139, 2019.
8. Paolicelli RC, Sierra A, Stevens B, Tremblay ME, Aguzzi A, Ajami B, Amit I, Audinat E, Bechmann I, Bennett M, *et al*: Microglia states and nomenclature: A field at its crossroads. Neuron 110: 3458-3483, 2022.
9. Parajuli B and Koizumi S: Strategies for manipulating microglia to determine their role in the healthy and diseased brain. Neurochem Res 48: 1066-1076, 2023.
10. Freyermuth-Trujillo X, Segura-Uribe JJ, Salgado-Ceballos H, Orozco-Barrios CE and Coyoy-Salgado A: Inflammation: A target for treatment in spinal cord injury. Cells 11: 2692, 2022.
11. Deng J, Meng F, Zhang K, Gao J, Liu Z, Li M, Liu X, Li J, Wang Y, Zhang L and Tang P: Emerging roles of microglia depletion in the treatment of spinal cord injury. Cells 11: 1871, 2022.
12. Devanney NA, Stewart AN and Gensel JC: Microglia and macrophage metabolism in CNS injury and disease: The role of immunometabolism in neurodegeneration and neurotrauma. Exp Neurol 329: 113310, 2020.
13. Shields DC, Haque A and Banik NL: Neuroinflammatory responses of microglia in central nervous system trauma. J Cereb Blood Flow Metab 40: S25-S33, 2020.
14. Mesquida-Veny F, Del Rio JA and Hervera A: Macrophagic and microglial complexity after neuronal injury. Prog Neurobiol 200: 101970, 2021.
15. Verkhratsky A, Sun D and Tanaka J: Snapshot of microglial physiological functions. Neurochem Int 144: 104960, 2021.
16. Savill J and Fadok V: Corpse clearance defines the meaning of cell death. Nature 407: 784-788, 2000.
17. Hochreiter-Hufford A and Ravichandran KS: Clearing the dead: Apoptotic cell sensing, recognition, engulfment, and digestion. Cold Spring Harb Perspect Biol 5: a008748, 2013.
18. Moon B, Yang S, Moon H, Lee J and Park D: After cell death: The molecular machinery of efferocytosis. Exp Mol Med 55: 1644-1651, 2023.
19. Doran AC, Yurdagul A Jr and Tabas I: Efferocytosis in health and disease. Nat Rev Immunol 20: 254-267, 2020.
20. Andrews SJ, Renton AE, Fulton-Howard B, Podlesny-Drabiniok A, Marcora E and Goate AM: The complex genetic architecture of Alzheimer's disease: Novel insights and future directions. EBioMedicine 90: 104511, 2023.
21. Balena T, Lillis K, Rahmati N, Bahari F, Dzhala V, Berdichevsky E and Staley K: A dynamic balance between neuronal death and clearance after acute brain injury. bioRxiv 14: 2023.02.14.528332, 2023.
22. Mike JK and Ferriero DM: Efferocytosis mediated modulation of injury after neonatal brain hypoxia-ischemia. Cells 10: 1025, 2021.
23. Ortuno FM, Torres C, Glosekotter P and Rojas I: New trends in biomedical engineering and bioinformatics applied to biomedicine-special issue of IWBBIO 2014. Biomed Eng Online 14 (Suppl 2): I1, 2015.
24. van Dijk EL, Auger H, Jaszczyszyn Y and Thermes C: Ten years of next-generation sequencing technology. Trends Genet 30: 418-426, 2014.
25. Greener JG, Kandathil SM, Moffat L and Jones DT: A guide to machine learning for biologists. Nat Rev Mol Cell Biol 23: 40-55, 2022.
26. Masuda T, Sankowski R, Staszewski O and Prinz M: Microglia heterogeneity in the single-cell era. Cell Rep 30: 1271-1281, 2020.
27. Grommes C, Lee CY, Wilkinson BL, Jiang Q, Koenigsknecht-Talboo JL, Varnum B and Landreth GE: Regulation of microglial phagocytosis and inflammatory gene expression by Gas6 acting on the Axl/Mer family of tyrosine kinases. J Neuroimmune Pharmacol 3: 130-140, 2008.
28. Ji R, Tian S, Lu HJ, Lu Q, Zheng Y, Wang X, Ding J, Li Q and Lu Q: TAM receptors affect adult brain neurogenesis by negative regulation of microglial cell activation. J Immunol 191: 6165-6177, 2013.
29. Scott RS, McMahon EJ, Pop SM, Reap EA, Caricchio R, Cohen PL, Earp HS and Matsushima GK: Phagocytosis and clearance of apoptotic cells is mediated by MER. Nature 411: 207-211, 2001.
30. Healy LM, Perron G, Won SY, Michell-Robinson MA, Rezk A, Ludwin SK, Moore CS, Hall JA, Bar-Or A and Antel JP: MerTK is a functional regulator of myelin phagocytosis by human myeloid cells. J Immunol 196: 3375-3384, 2016.
31. Fourgeaud L, Traves PG, Tufail Y, Leal-Bailey H, Lew ED, Burrola PG, Callaway P, Zagórska A, Rothlin CV, Nimmerjahn A and Lemke G: TAM receptors regulate multiple features of microglial physiology. Nature 532: 240-244, 2016.
32. Christoph S, Deryckere D, Schlegel J, Frazer JK, Batchelor LA, Trakhimets AY, Sather S, Hunter DM, Cummings CT, Liu J, *et al*: UNC569, a novel small-molecule mer inhibitor with efficacy against acute lymphoblastic leukemia in vitro and in vivo. Mol Cancer Ther 12: 2367-2377, 2013.
33. Kalyan M, Tousif AH, Sonali S, Vichitra C, Sunanda T, Praveenraj SS, Ray B, Gorantla VR, Rungratanawanich W, Mahalakshmi AM, *et al*: Role of endogenous lipopolysaccharides in neurological disorders. Cells 11: 4038, 2022.
34. Brown GC, Camacho M and Williams-Gray CH: The endotoxin hypothesis of Parkinson's disease. Mov Disord 38: 1143-1155, 2023.
35. Atta AA, Ibrahim WW, Mohamed AF and Abdelkader NF: Microglia polarization in nociplastic pain: Mechanisms and perspectives. Inflammopharmacology 31: 1053-1067, 2023.
36. Zhou X, Zhao R, Lv M, Xu X, Liu W, Li X, Gao Y, Zhao Z, Zhang Z, Li Y, *et al*: ACSL4 promotes microglia-mediated neuroinflammation by regulating lipid metabolism and VGLL4 expression. Brain Behav Immun 109: 331-343, 2023.
37. Wang M, Yang Y, Guo Y, Tan R, Sheng Y, Chui H, Chen P, Luo H, Ying Z, Li L, *et al*: Xiaoxuming decoction cutting formula reduces LPS-stimulated inflammation in BV-2 cells by regulating miR-9-5p in microglia exosomes. Front Pharmacol 14: 1183612, 2023.
38. Wu J, Han Y, Xu H, Sun H, Wang R, Ren H and Wang G: Deficient chaperone-mediated autophagy facilitates LPS-induced microglial activation via regulation of the p300/NF-κB/NLRP3 pathway. Sci Adv 9: eadi8343, 2023.

39. He Y, Wang Y, Yu H, Tian Y, Chen X, Chen C, Ren Y, Chen Z, Ren Y, Gong X, *et al*: Protective effect of Nr4a2 (Nurr1) against LPS-induced depressive-like behaviors via regulating activity of microglia and CamkII neurons in anterior cingulate cortex. Pharmacol Res 191: 106717, 2023.
40. Noristani HN, Gerber YN, Sabourin JC, Le Corre M, Lonjon N, Mestre-Frances N, Hirbec HE and Perrin FE: RNA-Seq analysis of microglia reveals time-dependent activation of specific genetic programs following spinal cord injury. Front Mol Neurosci 10: 90, 2017.
41. Leek JT, Johnson WE, Parker HS, Jaffe AE and Storey JD: The sva package for removing batch effects and other unwanted variation in high-throughput experiments. Bioinformatics 28: 882-883, 2012.
42. Ritchie ME, Phipson B, Wu D, Hu Y, Law CW, Shi W and Smyth GK: limma powers differential expression analyses for RNA-sequencing and microarray studies. Nucleic Acids Res 43: e47, 2015.
43. Langfelder P and Horvath S: WGCNA: An R package for weighted correlation network analysis. BMC Bioinformatics 9: 559, 2008.
44. Horvath S and Dong J: Geometric interpretation of gene coexpression network analysis. PLoS Comput Biol 4: e1000117, 2008.
45. Wang H and Zhou L: Random survival forest with space extensions for censored data. Artif Intell Med 79: 52-61, 2017.
46. Han H, Lee S and Lee I: NGSEA: Network-based gene set enrichment analysis for interpreting gene expression phenotypes with functional gene sets. Mol Cells 42: 579-588, 2019.
47. Wu T, Hu E, Xu S, Chen M, Guo P, Dai Z, Feng T, Zhou L, Tang W, Zhan L, *et al*: clusterProfiler 4.0: A universal enrichment tool for interpreting omics data. Innovation (Camb) 2: 100141, 2021.
48. Zhou Y, Zhou B, Pache L, Chang M, Khodabakhshi AH, Tanaseichuk O, Benner C and Chanda SK: Metascape provides a biologist-oriented resource for the analysis of systems-level datasets. Nat Commun 10: 1523, 2019.
49. Jeong H, Mason SP, Barabasi AL and Oltvai ZN: Lethality and centrality in protein networks. Nature 411: 41-42, 2001.
50. Ito K and Murphy D: Application of ggplot2 to pharmacometric graphics. CPT Pharmacometrics Syst Pharmacol 2: e79, 2013.
51. Tibshirani R, Bien J, Friedman J, Hastie T, Simon N, Taylor J and Tibshirani RJ: Strong rules for discarding predictors in lasso-type problems. J R Stat Soc Series B Stat Methodol 74: 245-266, 2012.
52. Orihuela R, McPherson CA and Harry GJ: Microglial M1/M2 polarization and metabolic states. Br J Pharmacol 173: 649-665, 2016.
53. Livak KJ and Schmittgen TD: Analysis of relative gene expression data using real-time quantitative PCR and the 2(-Delta Delta C(T)) method. Methods 25: 402-408, 2001.
54. Nomura K, Vilalta A, Allendorf DH, Hornik TC and Brown GC: Activated microglia desialylate and phagocytose cells via neuraminidase, galectin-3, and mer tyrosine kinase. J Immunol 198: 4792-4801, 2017.
55. Barberis E, Khoso S, Sica A, Falasca M, Gennari A, Dondero F, Afantitis A and Manfredi M: Precision medicine approaches with metabolomics and artificial intelligence. Int J Mol Sci 23: 11269, 2022.
56. Sanchez-Baizan N, Ribas L and Piferrer F: Improved biomarker discovery through a plot twist in transcriptomic data analysis. BMC Biol 20: 208, 2022.
57. Liu T, Wang Y, Wang Y, Cheung SK, Or PM, Wong CW, Guan J, Li Z, Yang W, Tu Y, *et al*: The mitotic regulator RCC2 promotes glucose metabolism through BACH1-dependent transcriptional upregulation of hexokinase II in glioma. Cancer Lett 549: 215914, 2022.
58. Yan L, Fu J, Dong X, Chen B, Hong H and Cui Z: Identification of hub genes in the subacute spinal cord injury in rats. BMC Neurosci 23: 51, 2022.
59. Alhamzawi R and Ali HTM: The Bayesian adaptive lasso regression. Math Biosci 303: 75-82, 2018.
60. Zhao J, Zhang W, Wu T, Wang H, Mao J, Liu J, Zhou Z, Lin X, Yan H and Wang Q: Efferocytosis in the central nervous system. Front Cell Dev Biol 9: 773344, 2021.
61. Poon IKH and Ravichandran KS: Targeting efferocytosis in inflammaging. Annu Rev Pharmacol Toxicol 23: 339-357, 2023.
62. Nagata S: Apoptosis and clearance of apoptotic cells. Annu Rev Immunol 36: 489-517, 2018.
63. Zhou L and Matsushima GK: Tyro3, Axl, Mertk receptor-mediated efferocytosis and immune regulation in the tumor environment. Int Rev Cell Mol Biol 361: 165-210, 2021.
64. Wang CY and Lin CF: Annexin A2: Its molecular regulation and cellular expression in cancer development. Dis Markers 2014: 308976, 2014.
65. Christensen MV, Hogdall CK, Jochumsen KM and Hogdall EVS: Annexin A2 and cancer: A systematic review. Int J Oncol 52: 5-18, 2018.
66. Mickleburgh I, Burtle B, Hollas H, Campbell G, Chrzanowska-Lightowlers Z, Vedeler A and Hesketh J: Annexin A2 binds to the localization signal in the 3' untranslated region of c-myc mRNA. FEBS J 272: 413-421, 2005.
67. Grewal T, Wason SJ, Enrich C and Rentero C: Annexins-insights from knockout mice. Biol Chem 397: 1031-1053, 2016.
68. Wang T, Wang Z, Niu R and Wang L: Crucial role of Anxa2 in cancer progression: Highlights on its novel regulatory mechanism. Cancer Biol Med 16: 671-687, 2019.
69. Mayran N, Parton RG and Gruenberg J: Annexin II regulates multivesicular endosome biogenesis in the degradation pathway of animal cells. EMBO J 22: 3242-3253, 2003.
70. Zobiack N, Rescher U, Ludwig C, Zeuschner D and Gerke V: The annexin 2/S100A10 complex controls the distribution of transferrin receptor-containing recycling endosomes. Mol Biol Cell 14: 4896-4908, 2003.
71. Navines-Ferrer A and Martin M: Long-tailed unconventional class I myosins in health and disease. Int J Mol Sci 21: 2555, 2020.
72. Giron-Perez DA, Vadillo E, Schnoor M and Santos-Argumedo L: Myo1e modulates the recruitment of activated B cells to inguinal lymph nodes. J Cell Sci 133: jcs235275, 2020.
73. Zhang Y, Du W, Chen Z and Xiang C: Upregulation of PD-L1 by SPP1 mediates macrophage polarization and facilitates immune escape in lung adenocarcinoma. Exp Cell Res 359: 449-457, 2017.
74. Yim A, Smith C and Brown AM: Osteopontin/secreted phosphoprotein-1 harnesses glial-, immune-, and neuronal cell ligand-receptor interactions to sense and regulate acute and chronic neuroinflammation. Immunol Rev 311: 224-233, 2022.
75. Rosmus DD, Lange C, Ludwig F, Ajami B and Wieghofer P: The role of osteopontin in microglia biology: Current concepts and future perspectives. Biomedicines 10: 840, 2022.
76. De Schepper S, Ge JZ, Crowley G, Ferreira LSS, Garceau D, Toomey CE, Sokolova D, Rueda-Carrasco J, Shin SH, Kim JS, *et al*: Perivascular cells induce microglial phagocytic states and synaptic engulfment via SPP1 in mouse models of Alzheimer's disease. Nat Neurosci 26: 406-415, 2023.
77. Andoh M and Koyama R: Comparative review of microglia and monocytes in CNS phagocytosis. Cells 10: 2555, 2021.
78. Fang YP, Qin ZH, Zhang Y and Ning B: Implications of microglial heterogeneity in spinal cord injury progression and therapy. Exp Neurol 359: 114239, 2023.
79. Kroner A and Almanza JA: Role of microglia in spinal cord injury. Neurosci Lett 709: 134370, 2019.